9-1-2013

Nonequilibrium heterogeneous catalysis in the long mean-free-path regime

D. P. Sheehan

University of San Diego, dsheehan@sandiego.edu

Nonequilibrium heterogeneous catalysis in the long mean-free-path regime

D. P. Sheehan[*]

Department of Physics, University of San Diego, San Diego, California 92110, USA
(Received 26 March 2013; published 18 September 2013)

It is shown that a standard principle of traditional catalysis—that a catalyst does not alter the final thermodynamic equilibrium of a reaction—can fail in low-pressure, heterogeneous gas-surface reactions. Kinetic theory for this *epicatalysis* is presented, and two well-documented experimental examples are detailed: surface ionized plasmas and hydrogen dissociation on refractory metals. This phenomenon should be observable over a wide range of temperatures and pressures, and for a broad spectrum of heterogeneous reactions. By transcending some constraints of equilibrium thermodynamics, epicatalysis might provide additional control parameters and synthetic routes for reactions, and enable product streams boosted in thermochemical energy or desirable species.

I. INTRODUCTION

Catalysis is the axis around which the biological and modern industrial worlds turn [1–3]. Virtually all of biochemistry is mediated by catalysts (e.g., enzymes and abzymes). Life itself has been characterized as a self-replicating, thermodynamically open, autocatalytic network of reactions [4]. Industrially, more than 90% of all products involve catalysts at some stage in their production [5]. The most consequential are gas-solid heterogeneous catalysts, for the synthesis of chemical feedstocks (e.g., ammonia, methanol, sulfuric acid), and the transformation of hydrocarbons (e.g., cracking, reformation, oxidation, isomerization, hydrogenation). To highlight just one, the Haber-Bosch ammonia synthesis has influenced civilization perhaps more than any other over the last century [6]. Annually, it consumes 3%–5% of the world's natural gas and 1%–2% of its total energy. The yearly production of ammonia is on par with the entire mass of humanity. Roughly half of the protein in a typical human body has nitrogen fixed by this process. Ammonia-based fertilizers sustain 30%–40% of the world's population, and arguably, more than three billion of the world's seven billion people would not be alive today without them [6].

Traditional (positive) catalysts satisfy three general principles. First, they increase reaction rates by providing lower activation energies for rate-limiting steps. Second, they are not consumed by their net reactions although they are intimately involved in them. Third, they do not alter final thermodynamic equilibria.

In this paper it is shown that principle 3 can break down in heterogeneous gas-surface reactions. To differentiate it from traditional catalysis, this phenomenon will be called *epicatalysis*. It emerges out of standard kinetic theory in the limit of low gas number density (pressure) and strong gas-surface interactions. This article opens (Sec. II) with an unambiguous and extensively documented experimental example of epicatalysis that has been hiding in plain sight for over 50 years: surface ionized plasmas [7,8]. Next, the kinetic basis for epicatalysis is introduced (Sec. III), followed by a purely chemical example (Sec. IV): hydrogen dissociation on high-temperature refractory metals [9–11]. The paper concludes with a discussion of the potential strengths and limitations of epicatalysis (Sec. V).

II. SURFACE IONIZED PLASMAS

Plasmas are created by a variety of mechanisms, literally any process that can separate an electron from its host species: e.g., particle beams; uv or x rays; intense electric fields (e.g., lasers). Virtually all involve nonequilibrium (nonthermal) processes in thermodynamically *open* systems. In contradistinction, here we consider and contrast two well-studied mechanisms for generating gaseous plasmas under *thermal*, *closed* blackbody cavity conditions: (a) collisional ionization (CI) and (b) surface ionization (SI) [12,13]. The first (CI) creates plasmas via thermal collisions and is consistent with standard gas phase equilibrium, while the second (SI) relies on strong gas-surface interactions and evidences epicatalysis. Both can be expressed with the generic reaction $M \rightleftharpoons M^+ + e^-$, where M is a neutral ionizable species. Whereas CI plasmas conform to traditional expectations of thermal equilibrium (spatially uniform, isothermal, Maxwellian velocity distributions with $T_M = T_{M^+} = T_{e^-}$; ionization ratios conforming to the Saha relation), SI plasmas do not. Rather, SI plasmas can exhibit strongly nonequilibrium features, including non-Maxwellian, beamlike ion velocity distributions (for which temperature is not well defined), and suprathermally high ionization ratios. These nonequilibrium features, which derive directly from SI's gas-surface interactions, can be maintained indefinitely under blackbody cavity conditions. To appreciate their counterintuitive nature, we begin with the more familiar CI plasmas.

A. Collisionally ionized plasmas

Consider a sealed, isothermal blackbody cavity with chemically inert walls, containing gaseous species M. For the sake of this discussion, and for later comparison, we consider the alkali metal cesium (Cs), which is easily vaporized (the melting point is 301 K and the boiling point 944 K), and is relatively easy to ionize, having a small ionization potential ($V_I = 3.9$ eV). Because the cavity walls are physically and chemically inert with respect to Cs, the atoms behave as an ideal gas, interacting solely via collisions (gas-gas, gas-wall). At cavity temperature T and volume number density n, the ratio of ionized to neutral atoms ($\chi_{CI} \equiv \frac{n_i}{n_o}$) is given by the

_____
[*]dsheehan@sandiego.edu

Saha relation [14]: $\chi_{\mathrm{CI}} \equiv \frac{n_i}{n_o} = \frac{2}{\Lambda_{\mathrm{dB}}} \frac{g_i}{g_o} \frac{1}{n_e} \exp[-\frac{V_I}{kT}]$. Here Λ_{dB} is the thermal de Broglie wavelength $\Lambda_{\mathrm{dB}} = (\frac{2\pi\hbar^2}{m_e kT})^{1/2}$; kT is the thermal energy; m_e is the electron mass; $n_{o,i,e}$ are the neutral atom, ion, and electron volume number densities; and g_i/g_o is the ratio of statistical weights for the ion and neutral species (for Cs, $\frac{g_i}{g_o} = 1/2$).

At standard temperature and pressure (STP), ionization ratios χ_{CI} are small. For Cs at STP, one has $\chi_{\mathrm{CI}}(\mathrm{Cs}; \mathrm{STP}) \simeq 10^{-36}$, meaning that even in a $(1 \text{ km})^3$-sized cavity filled with Cs gas at STP, not even one atom would likely be ionized. On the other hand, at high temperature and reduced number density, χ_{CI} increases substantially. As a second example—and one that will be useful for comparison with SI plasmas—consider Cs ($T = 2000$ K and $n_o = 10^{17}$ m^{-3}). In this case, $\chi_{\mathrm{CI}}(\mathrm{Cs}; 2000$ K$) \simeq 0.3$, meaning that this gas is roughly 25% ionized under blackbody cavity conditions: a legitimate plasma.

For CI plasmas, Cs atoms ionize strictly via collisions among themselves and with the blackbody cavity walls; therefore, the neutral, ion, and electron populations follow Maxwell-Boltzmann statistics, i.e., $f(v)dv = N(\frac{m}{2\pi kT})^{1/2} \exp[-\frac{mv^2}{2kT}]dv$. To first approximation the CI plasma is a three-component ideal gas. The walls of the blackbody cavity play no explicit role in the character of the plasma and, for practical purposes, they can be ignored.

Taking the CI plasma as the template for thermodynamic equilibrium, we now turn to surface ionized plasmas, in particular, to a workhorse of plasma physics, the Q plasma.

B. Q plasmas

Q plasmas have been testbeds for basic plasma physics for over 50 years [7,8,15,16]. They are created through surface ionization of low-ionization-potential metal vapor atoms (typically alkali metal or alkaline earth metal vapors, e.g., K,Cs,Ba) on high-work-function refractory metal hotplates (e.g., W,Ta,Re), as depicted in Fig. 1. If the hotplate work function exceeds the ionization potential of the metal vapor atoms ($\Phi > V_I$), the vapor atoms impinging on the hotplate preferentially release one of their valence electrons into the Fermi sea of the metal, becoming positive ions. At elevated temperatures ($T \gtrsim 2000$ K), they can evaporate.

Meanwhile, electrons are thermionically emitted from the high-temperature hotplate via Richardson emission and create a negative space charge layer (electrostatic sheath) over the surface, which accelerates the positive ions off the hotplate up to supersonic speeds. The thermionically emitted electrons, space charge neutralized by the supersonically departing ions, can now freely leave the surface without electrostatic impediment. The net result is an electron-ion plasma streaming away from the hotplate surface. A strong axial magnetic field typically confines the plasma. For a double-ended Q plasma [Fig. 1(a)], the two hotplates represent the boundary walls of the blackbody cavity, as well as electrical ground. In fact, the magnetic field and long cylindrical geometry are unnecessary; Q plasmas can form in unmagnetized, three-dimensional blackbody cavities.

Research grade Q plasmas are usually a few centimeters in diameter and up to several meters in length. They are
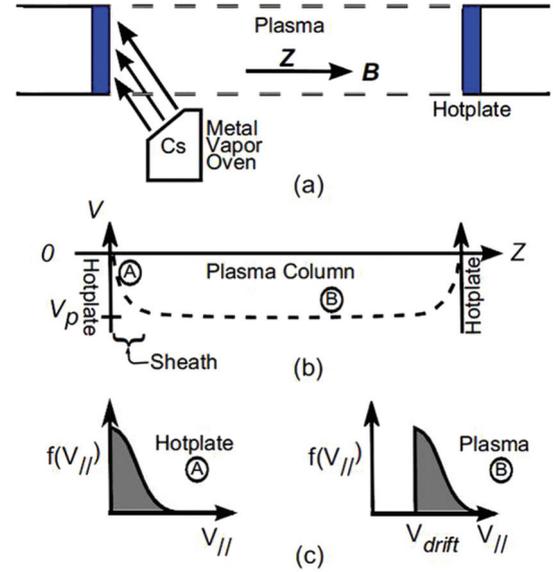

FIG. 1. (Color online) Q plasmas. (a) Schematic of double-ended Q machine. (b) Electrostatic potential profile axially along the electron-rich plasma column. (c) Ion parallel velocity distributions for Q plasma at the hotplate (A) and in the plasma bulk (B).

sufficiently rarified ($n \lesssim 10^{17}$ m^{-3}) that recombinative collisions are usually ignorable [17]. Hotplates are commonly heated via electron bombardment, but other modes are possible (e.g., blackbody radiation, induction, and Ohmic heating) [7].

The composition of the walls (hotplate) determines the primary characteristics of a Q plasma; these include (a) plasma density, (b) plasma potential, and (c) ion velocity distributions. The number density (n) is determined by the quantity and species of the metal vapor, as well as by the temperature (T) and work function (Φ) of the hotplate. The fractional ionization of the metal vapor on the hotplate surface is given by the Saha-Langmuir relation [12] $\chi_{\mathrm{SI}} \equiv \frac{n_i}{n_o} = \frac{g_i}{g_o} \exp[\frac{(e\Phi - V_I)}{kT}]$. Notice that, unlike the Saha relation for CI plasmas, the Saha-Langmuir relation explicitly involves the wall (surface) composition, via Φ. This marks surface ionization as epicatalysis.

The Q plasma's ionization ratio depends crucially on the work function. Consider, for example, χ_{SI} for Cs ($V_I = 3.9$ V) on each of four refractory metals, at $T = 2000$ K. They are $\chi_{\mathrm{SI}}(\mathrm{Ta}; \Phi = 4.1$ V$) = 1.6$, $\chi_{\mathrm{SI}}(\mathrm{Mo}; \Phi = 4.2$ V$) = 2.8$, $\chi_{\mathrm{SI}}(\mathrm{W}; \Phi = 4.6$ V$) = 29$, and $\chi_{\mathrm{SI}}(\mathrm{Re}; \Phi \simeq 5$ V$) \simeq 300$. Assuming these ionization ratios are reflected in the plasmas emanating from the surfaces—a feature that has been verified experimentally [18,19]—the ionization ratio of the plasma is surface dependent. In contrast, recall that if no metal is present (i.e., $\Phi = 0$), and if ionization proceeds solely by thermal collisions, then the Saha relation predicts only $\chi_{\mathrm{CI}} = 0.3$. In summary, Q plasmas can be much more highly ionized than CI plasmas ($\chi_{\mathrm{SI}} \gg \chi_{\mathrm{CI}}$).

The plasma electron number density is set by Richardson emission, which also depends on the surface work function, i.e., $J_{\mathrm{Rich}} = AT^2 \exp(-\frac{e\Phi}{kT}) \exp(\frac{eV_p}{kT})$, where J_{Rich} is the Richardson current density, A is the Richardson constant for pure metals (6×10^5–12×10^5 A/m^2 K^2); and V_p is the *plasma potential*. Plasmas normally reside at nonzero

electrostatic potentials with respect to their confining walls (ground). The plasma potential is determined by the net charge of the plasma, which in turn is set by the relative fluxes of electrons and positive ions into and out of the plasma volume. Q plasmas are normally operated in the electron-rich regime, wherein the Richardson current dominates the thermal electron current ($J_{\text{Rich}} > J_{\text{thermal}} = \frac{e n_e v_{\text{thermal}}}{4}$), where $v_{\text{thermal}} = \sqrt{8kT/\pi m_e}$ is the average electron thermal speed. Electron-rich plasmas exhibit negative plasma potentials ($V_p < 0$); ion-rich plasmas, with $V_p > 0$, are also possible. Typical values of V_p range up to a few volts. Figure 1(b) depicts the spatial structure of V_p along the plasma column for an electron-rich plasma.

The plasma potential is established between the walls (ground) and the plasma bulk over a thin but macroscopic region near the hotplate called the plasma sheath. Within the sheath, electric fields can be substantial (e.g., 10^3–10^4 V/m). It is characterized by asymmetric particle fluxes, non-Maxwellian ion distributions, and electric fields that supersonically accelerate ions into the bulk plasma.

Owing to V_p and the sheath, ion velocity distributions in Q plasmas are non-Maxwellian in the direction parallel to the sheath electric field (and confining magnetic field), while retaining their Maxwellian profile in the perpendicular direction [Fig. 1(c)]. They would retain their non-Maxwellian nature in three-dimensional, unmagnetized cavities. Their parallel drift speed ($v_d = \sqrt{2eV_p/m_i}$) can be several times the ion thermal speed such that the ion velocity distribution is beamlike. This beamlike character has been verified by electrostatic-grid particle velocity analyzers and via laser-induced fluorescence measurements [7]. If the plasma is noncollisional, which is the case for plasma densities at or below about $n_i \simeq 10^{15}$ m^{-3}, this non-Maxwellian distribution persists throughout the plasma bulk, as indicated in Fig. 1(c). At these low densities, the scale of three-body recombinative collisions between ions and electrons is many times the length of the plasma column, so plasma composition does not vary appreciably throughout the bulk. Even at higher densities ($n \sim 10^{17}$ m^{-3}), plasma recombination is usually not a serious issue.

Q plasmas satisfy the criteria for epicatalysis. First, behaving as catalysts, the hotplate surfaces speed the ionization-recombination reaction ($M \rightleftharpoons M^+ + e^-$) and, second, they are not consumed. (A tungsten hotplate can operate for years without appreciable degradation, aside from recrystallization.). However, hotplates break the third principle of catalysis by generating a strongly nonequilibrium gas phase that is directly linked to a surface property (Φ), as detailed above.

Q plasmas and CI plasmas exist along a thermodynamic continuum. At low number densities (and physically active surfaces, $\Phi > V_I$) epicatalytic Q plasmas arise, whereas at higher number densities, where recombinative gas phase collisions prevail, CI plasmas emerge. In principle, both plasmas can coexist in the same blackbody cavity, with Q plasmas near the walls, transitioning to CI plasmas in the interior.

To summarize, Q plasmas have no independent existence apart from the properties of their boundary (hotplate) surfaces. Long standing theory and experimental measurements confirm that their signature features (e.g., high ionization ratio, nonzero plasma potential, and beamlike ion velocity distributions) are

nonequilibrium in character, that they extend throughout the plasma column, and that they depend strongly on the work function and temperature of the boundary hotplates. Q plasmas represent a nonequilibrium stationary state under blackbody cavity conditions. They are examples of epicatalysis.

III. THEORY

In this section the basic theory of epicatalysis is developed, using as a touchstone the generic dissociation reaction ($A_2 \rightleftharpoons 2A$), which applies both to Q plasmas [7,8,14] and to hydrogen-metal systems (Sec. IV). Limiting cases of this reaction are examined, and it is shown that epicatalysis arises in the long mean-free-path regime for heterogeneous catalysis.

A. Kinetic theory

Epicatalysis emerges naturally from the standard kinetic formalism describing heterogeneous gas-surface systems, when the following two criteria are met:

Criterion 1. The gas species chemically or physically interact strongly with the surface and desorb in concentrations not reflecting standard gas phase equilibrium.

Criterion 2. Gas phase reactions are sufficiently rare that equilibrium cannot be established in this phase.

Examples of criterion 1 include (a) surface ionization of Groups IA and IIA metal atoms (e.g., K,Cs,Ba) on high-work-function metals (e.g., W,Re,Pt) [12,13], e.g., Q plasmas (Sec. II); and (b) dissociation of light molecules (e.g., H_2,N_2,O_2,CO_2) on transition metals [3,20,21]. Criterion 2 is met in the low-number-density (-pressure) regime. Let λ_{Rx} be the mean free path for a gas phase chemical reaction, and let L be the effective distance between gas-surface interactions, usually taken to be the size of the reaction chamber. Criterion 2 can be written as $\lambda_{\text{Rx}} \gtrsim L$. Because λ_{Rx} scales inversely with number density (n), Criterion 2 can be satisfied in the low-n (low-pressure) regime for macroscopic reaction volumes (L large), or in the high-n (high-pressure) regime for microscopic ones (L small). Industrial catalysts rarely, if ever, satisfy criterion 2 because they typically operate in high-pressure macroscopic chambers, where $\lambda_{\text{Rx}} \ll L$.

As a touchstone for discussion, consider the archetypal heterogeneous reaction ($A_2 \rightleftharpoons 2A$), depicted in Fig. 2. So that its thermodynamics is well defined, let the reaction be confined to a sealed (closed) isothermal blackbody cavity. Gas and surface phases coexist stably here, but equilibrium is not assumed. The only physical processes assumed are dissociation, two-body recombination, adsorption, and desorption.
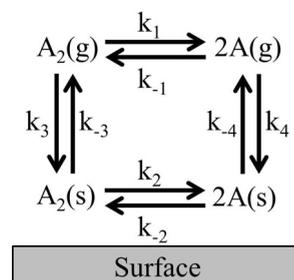

FIG. 2. Gas and surface reactions for $A_2 \rightleftharpoons 2A$.

The full set of kinetic equations for the gas (g) and surface (s) phases (Fig. 2) are appropriate because epicatalysis does not presume equilibrium. Referring to Fig. 2, the kinetic equations are

$$D_t[A_2(g)] \equiv \frac{d[A_2(g)]}{dt} = -k_1[A_2(g)] + k_{-1}[A(g)]^2 - k_3[A_2(g)] + k_{-3}[A_2(s)],$$

$$D_t[A(g)] \equiv \frac{d[A(g)]}{dt} = +k_1[A_2(g)] - k_{-1}[A(g)]^2 - k_4[A(g)] + k_{-4}[A(s)],$$

$$D_t[A_2(s)] \equiv \frac{d[A_2(s)]}{dt} = -k_2[A_2(s)] + k_{-2}[A(s)]^2 + k_3[A_2(g)] - k_{-3}[A_2(s)],$$

$$D_t[A(s)] \equiv \frac{d[A(s)]}{dt} = +k_2[A_2(s)] - k_{-2}[A(s)]^2 + k_4[A(g)] - k_{-4}[A(s)].$$

(1)

These can be recast in matrix form as

$$D_t\mathbf{A} \equiv \frac{d}{dt}\mathbf{A} = \mathbf{T}\mathbf{A} = \begin{bmatrix} -(k_1+k_3) & k_{-1}[A(g)] & k_{-3} & 0 \\ k_1 & -\{k_{-1}[A(g)]+k_4\} & 0 & k_{-4} \\ k_3 & 0 & -(k_2+k_{-3}) & k_{-2}[A(s)] \\ 0 & k_4 & k_2 & -\{k_{-2}[A(s)]+k_{-4}\} \end{bmatrix} \begin{bmatrix} A_2(g) \\ A(g) \\ A_2(s) \\ A(s) \end{bmatrix}.$$

(2)

Here **A** is the vector composed of the gas and surface species concentrations, and **T** is the nonlinear transition matrix, which drives the time-changing concentrations, $\frac{d}{dt}\mathbf{A} \equiv D_t\mathbf{A}$. The heuristic structure of **T** is revealing:

$$\mathbf{T} = \begin{bmatrix} \begin{pmatrix} T_{11} & T_{12} \\ T_{21} & T_{22} \end{pmatrix} & \begin{pmatrix} T_{13} & T_{14} \\ T_{23} & T_{24} \end{pmatrix} \\ \begin{pmatrix} T_{31} & T_{32} \\ T_{41} & T_{42} \end{pmatrix} & \begin{pmatrix} T_{33} & T_{34} \\ T_{43} & T_{44} \end{pmatrix} \end{bmatrix} \equiv \begin{bmatrix} \text{(gas phase)} & \text{(adsorption)} \\ \text{(desorption)} & \text{(surface phase)} \end{bmatrix}.$$

(3)

T consists of four 2×2 submatrices. Its off-diagonal submatrices pertain solely to adsorption and desorption, while the diagonal submatrices describe interactions of each phase individually. The general solution to this set of four coupled, first-order, nonlinear differential equations is likewise nonlinear. For the experimental examples of epicatalysis in Secs. II and IV, the rate equations are even more nonlinear than they appear in Eqs. (1) because for them gas phase dissociation and recombination are two-body and three-body processes, respectively. The pertinent dissociation-recombination reaction equation is $A_2 + X \rightleftharpoons 2A + X$, where X is a third gas species (either A or A_2). The first two rate equations in (1) are thus modified by additional concentration terms $[X]$, raising their orders by 1.

Although solutions to the rate equations are nonlinear and usually analytically intractable, the following two limiting cases are key and easily derived.

1. Limiting case 1: Gas phase equilibrium

Let the surface phase be chemically inert and the gas phase be chemically active. That is, gas species do not interact with the surface, they merely adsorb and desorb from it. In this case, the transition matrix takes the form

$$\mathbf{T}_{\text{GPE}} = \begin{bmatrix} \text{(gas phase)} & \text{(adsorption)} \\ \text{(desorption)} & (\sim 0) \end{bmatrix},$$

and the reduced set of kinetic equations is easily solved. In the stationary state, when $D_t\mathbf{A} = 0$, as would evolve under closed blackbody cavity conditions, the limiting equations render standard gas phase equilibrium: $K_{\text{eq}}(g) \equiv \frac{k_1}{k_{-1}} = \frac{[A(g)]^2}{[A_2(g)]}$. This is a familiar and expected result. Often overlooked, however, are the surface phase concentrations. They are determined by the gas phase, linked by adsorption and desorption rate constants:

$$[A_2(s)]_{\text{neq}} = \frac{k_3}{k_{-3}}[A_2(g)]_{\text{eq}} \quad \text{and} \quad [A(s)]_{\text{neq}} = \frac{k_4}{k_{-4}}[A(g)]_{\text{eq}}.$$

(4)

The subscripts "eq" and "neq" stand for "equilibrium" and "nonequilibrium," indicating which concentrations are determined by an equilibrium constant. In this case, the gas phase concentrations (eq) are set by $K_{\text{eq}}(g)$ above, while the surface phase concentrations (neq) are not. Rather, the surface phase concentrations ($[A_2(s)]$ and $[A(s)]$) are set by the gas phase concentrations [Eq. (4)]. This is both reasonable and expected; after all, most everyday surfaces are chemically inert so their species concentrations closely follow the gas phases in which they are immersed. However, *a phase is a phase* so the following inverse case also holds.

2. Limiting case 2: Surface phase equilibrium (epicatalysis)

In this case, the inverse of case 1, the activities of the phases are reversed: the surface phase is chemically active, while the gas phase is chemically inert. The gas phase is rendered inert when the mean free path for gas phase reactions (λ_{Rx}) becomes very long compared with the effective size of the reaction chamber (L)—that is, $\lambda_{\text{Rx}} \gg L$—so that A and A_2 react only

with the surface (via adsorption, dissociation, desorption) and with each other *on* the surface (via recombination) [22]. Q plasmas (Sec. II) clearly satisfy these conditions.

For case 2 the transition matrix becomes

$$\mathbf{T}_{\text{SPE}} = \begin{bmatrix} (\sim 0) & (\text{Adsorption}) \\ (\text{Desorption}) & (\text{Surface Phase}) \end{bmatrix}.$$

Here the limiting equations for the stationary state ($D_t\mathbf{A} = 0$) render surface phase equilibrium—but not gas phase equilibrium; that is, $K_{\text{eq}}(s) = \frac{k_2}{k_{-2}} = \frac{[A(\text{s})]^2}{[A_2(\text{s})]}$. Now, in the reverse of case 1, the gas phase concentrations for case 2 are determined by the surface phase concentrations, again linked by the adsorption and desorption rate constants:

$$[A_2(\text{g})]_{\text{neq}} = \frac{k_{-3}}{k_3}[A_2(\text{s})]_{\text{eq}} \quad \text{and} \quad [A(\text{g})]_{\text{neq}} = \frac{k_{-4}}{k_4}[A(\text{s})]_{\text{eq}}. \tag{5}$$

Case 2 and Eq. (5) are the basis for epicatalysis. Principle 1 of catalysis is satisfied because the chemically active surface speeds up the reaction $A_2 \rightleftharpoons 2A$. Principle 2 is satisfied because the surface is not consumed in the reaction. Principle 3, however, is violated because the surface generates a gas phase that need not conform to gas phase equilibrium.

3. Intermediate regime

Epicatalysis is not an all-or-nothing phenomenon. Between limiting cases 1 and 2 is a nonlinear continuum. For this *intermediate* number density regime, where neither gas phase nor surface phase equilibrium is guaranteed, epicatalysis can be described qualitatively in terms of reaction rates. To satisfy criterion 1 the surface phase must be chemically active to an appreciable degree. This means surface dissociation and recombination rates ($k_2[A_2(\text{s})]$ and $k_{-2}[A(\text{s})]^2$), as well as the individual species desorption rates ($k_{-3}[A_2(\text{s})]$ and $k_{-4}[A(\text{s})]$), must be appreciable. Additionally, the desorption and adsorption rates must be such that the gas phase concentrations do not coincide with gas phase equilibrium. This is easily satisfied because, in general, gas and surface equilibrium constants are not equal $[K_{\text{eq}}(\text{g}) \neq K_{\text{eq}}(\text{s})]$ because their chemical environments are distinct. Moreover, equilibrium constants will be distinct between chemically and physically distinct surfaces, as well, so more generally, one can write: $(K_{\text{eq}}(\text{g}) \neq K_{\text{eq}}(\text{S1}) \neq K_{\text{eq}}(\text{S2}) \neq K_{\text{eq}}(\text{S3}) \neq \cdots)$. If so, then case 2 (epicatalysis) not only permits that, over a chemically active surface, the gas phase concentrations need not be those of gas phase equilibrium, it additionally allows that different nonequilibria gas phases can exist over chemically different surfaces (e.g., S1,S2,S3,...). This feature is experimentally manifest in the different ionization ratios for different vapor-hotplate combinations in the case of Q plasmas, as well as in the various metal combinations in hydrogen surface dissociation experiments (Sec. IV).

Returning to the intermediate case, criterion 2 requires that gas phase concentrations be significantly affected (preferably dominated) by surface desorption products. In terms of rate constants, this can be expressed as: $k_{-3}[A_2(\text{s})], k_{-4}[A(\text{s})] \gg k_1[A_2(\text{g})], k_{-1}[A(\text{g})]^2$. Toward which limit a particular system leans is determined by the degree to which its gas species
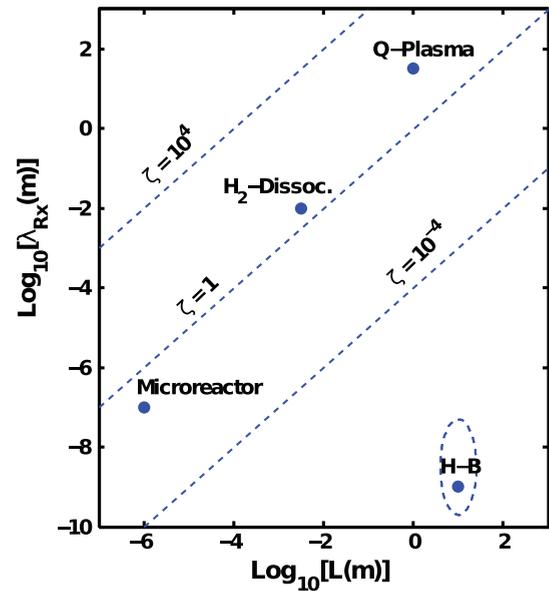

FIG. 3. (Color online) $\log_{10}(\lambda_{\text{Rx}})$ vs $\log_{10}(L)$ for representative epicatalytic and catalytic systems. Industrial heterogeneous catalysis thrives at $\zeta \ll 1$; the dotted ellipse circumscribes the range for typical reactors [Haber-Bosch (H-B):, $\zeta \sim 10^{-9}$]. Epicatalysis thrives in the vicinity of the $\zeta = 1$ trendline: Q plasmas (Sec. II); hydrogen dissociation (Re/W-H at 10 mTorr H_2) (Sec. IV); microreactor (1 atm). (Note: Two-body collisions are assumed for hydrogen dissociation.)

concentrations reflect gas phase versus surface phase reactions. An indicator of this is the ratio $\zeta \equiv \frac{\lambda_{\text{Rx}}}{L}$, derived from criterion 2 above. As ζ increases from zero, epicatalysis emerges, becomes robust in the range $\zeta \sim 1$, continues for $\zeta > 1$, and ultimately declines as further increases in λ_{Rx} signal number densities too low for epicatalytic surface effects to be thermodynamically significant.

Clearly, no real chemical system perfectly matches either limiting case. Nevertheless, both are good approximations to real and well-studied physical systems. Figure 3 plots catalytic and epicatalytic systems discussed in this paper versus λ_{Rx} and L. Epicatalytic systems Q plasmas (Sec. II) and hydrogen dissociation (Sec. IV) thrive in the vicinity of $\zeta \sim 1$, while industrial catalysts thrive at $\zeta \ll 1$. The Haber-Bosch process, for example, operates commercially at $\zeta \sim 10^{-9}$.

Epicatalysis is not merely a joint property of surfaces and gas species; it also depends critically on the number density and size of the system, as indicated through ζ. This means, for instance, that for a given surface type, gas load, and temperature, epicatalysis might be robust at one number density but insignificant at another. It might thrive in one section of a reaction vessel (probably near the walls), while being entirely absent in another, perhaps deep in the bulk gas phase, where $\zeta \ll 1$ is realized.

Epicatalysis raises a number of thermodynamic issues. First, it is emphasized that steady-state nonequilibrium gas phase concentrations over surfaces are common; they are, for instance, standard in gas flow reactors. Epicatalysis is distinct in that it allows stationary-state gas phase nonequilibrium in *closed* systems, e.g., under sealed isothermal blackbody cavity conditions.

Epicatalysis conforms to the principle of detailed balance [23], or at the level of individual particle trajectories, microscopic reversibility (reciprocity) [24,25]. In fact, it is predicated on them. Equation (5), the seminal relation characterizing epicatalysis, is obtained by appealing to detailed balance, specifically, by equating adsorption and desorption rates under the condition $D_t\mathbf{A} = 0$. At the level of individual particle trajectories, epicatalysis also adheres to the principle of microscopic reversibility (or *reciprocity* for gas-surface interactions) by similar reasoning. In contemplating this peculiar stationary state, it is not that a gas phase does not exist—for indeed it does—it is merely that its species concentrations are set by the surface phase because gas phase reactions are too rare to do so.

It is curious that epicatalysis was not identified long ago, given that heterogeneous catalysis has been studied and used extensively for more than a century. There might be several reasons for this. First, most chemists and physicists are trained to think in terms of thermodynamic equilibrium, rather than stationary-state nonequilibrium. Furthermore, thermodynamic arguments are usually framed in the thermodynamic limit, that is, to treat systems as spatially infinite, in the long time limit, free of boundary effects. These assumptions fail here. Epicatalysis depends on strong gas-surface interactions (criterion 1) as well as on finite system size and an inert gas phase (criterion 2), thereby confounding common thermodynamic expectations. Finally, in practice most commercial catalysis is carried out in large vessels at high pressures such that the $\zeta \gtrsim 1$ criterion for epicatalysis is not satisfied. The Haber-Bosch process, for instance, is typically conducted at 150–400 atm in vessels meters in size, and thus operates at $\zeta \sim 10^{-9}$ (Fig. 3). As a result, epicatalysis was unlikely to have been discovered accidentally via industrial catalysts. There are, of course, commercial devices that seem to rely inadvertently on epicatalysis (e.g., hydrogen atom sources). These, however, are niche markets whose research funding is usually inadequate for careful study of the underlying physical chemistry so, again, it was unlikely to have been discovered.

In summary, the full set of rate equations for gas and surface phase reactions ($A_2 \rightleftharpoons 2A$) is nonlinear. In the limit that the gas phase is active and the surface phase inert, gas phase equilibrium prevails. In the opposite limit, where the gas phase is inert and the surface phase active, surface phase equilibrium prevails and epicatalysis emerges [Eq. (5)]. In the intermediate regime, where both gas and surface phases are active to some degree, the extent of epicatalysis is determined by how closely the system hews to criteria 1 and 2.

IV. EPICATALYTIC HYDROGEN DISSOCIATION

In Sec. II, Q plasmas were identified as a clear-cut experimental example of epicatalysis. In this section, experimental evidence is presented for epicatalysis in the dissociation of low-pressure hydrogen on high-temperature transition metals. These results expand the reach of epicatalysis from the plasma realm to the much broader chemical regime.

Evidence for epicatalysis in surface-mediated hydrogen dissociation is scattered through the scientific literature, dating back at least to Langmuir, a century ago [9]. Here we focus on the most recent and stark examples. Based on experiments

conducted in the low-number-density regime, the consensus appears to be that (1) surface dissociation rates are distinct on different metals at otherwise identical temperatures, hydrogen pressures, and surface geometries; and (2) dissociation rates can be 1–2 orders of magnitude greater than those predicted by gas phase equilibrium. These observations are inconsistent with gas phase equilibrium thermodynamics, but they are signatures of epicatalysis. Discussion of these systems has been delayed until this section because their status is less clear-cut than is the case for Q plasmas. That is, experimentally they conform to the predictions of epicatalysis theory, but there is no single surface quantity analogous to Φ, as in the case of Q plasmas, to which to attribute their behavior. Quite to the contrary, heterogeneous reactions are notoriously dependent on multiple and often ill-defined physical variables [1–3].

A. Equilibrium gas phase

As in Sec. II contrasting CI and SI plasmas, here we contrast standard chemical gas phase equilibrium with that created via epicatalysis. The gas phase equilibrium constant $K_{eq}(g)$ can be calculated from kinetic rate constants ($k_{\pm 1}$ in Fig. 2) or from a Gibbs free energy change (ΔG) and T, via $K_{eq}(g) = \frac{k_1}{k_{-1}} = \exp(-\Delta G/RT)$. Many theoretically and experimentally derived rate constants have been proposed for hydrogen reactions. (See [26].) Equilibrium constants calculated from rate constants are model dependent and have limited temperature ranges of applicability. Here we will use $K_{eq}(g)$ derived from ΔG [26]. Returning to our benchmark temperature ($T = 2000$ K), these predict $K_{eq}(g) = 2.65 \times 10^{-6}$ molecules/cm^3, which indicates relatively little dissociation at 2000 K. Taking the stoichiometric partial pressure of H to be $2y \ll 1$, as indicated from K_{eq}, the dissociation ratio can be expressed as [27,28] $\chi_H \equiv \frac{[H]}{[H_2]} = \frac{2y}{1-y} \simeq 2y = \sqrt{K_{eq}(g)} = 1.63 \times 10^{-3}$. In other words, at 2000 K the partial pressure of hydrogen atoms and the dissociation ratio of the gas are very small. Figure 4 plots the dissociation ratio (χ_H) versus temperature over the range pertinent to the upcoming surveyed experiments (Sec. IV B1). The continuous curve is calculated from ΔG, while the individual points (labeled Re and W) are inferred from hydrogen-metal experiments (Sec. IV B1). Theoretical and experimental bridges between chemical systems like this and Q plasmas have been proposed [29,30].

B. Hydrogen-metal dissociation experiments

Most experiments that involve low-pressure, surface-mediated hydrogen dissociation were not specifically designed to study epicatalysis, so evidence for it is often indirect. We begin, however, with experiments especially designed to examine epicatalysis.

1. Surface comparison experiments [11,31,32]

Pairs of geometrically identical, pure metal filaments (W vs Mo and W vs Re) were tested side by side to compare their hydrogen dissociation rates at identical temperatures and partial pressures of hydrogen ($T \leqslant 2500$ K, $P \leqslant 30$ Torr). It was found that at low pressures and elevated temperatures hydrogen dissociation rates were distinct between different metals and significantly exceeded the predictions of gas
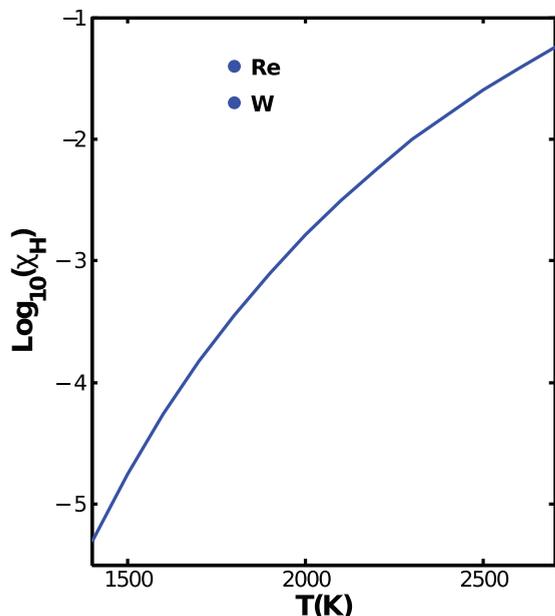
FIG. 4. (Color online) Dissociation ratio χ_H versus temperature for gas phase reaction $H_2 \rightleftharpoons 2H$. The solid curve corresponds to thermodynamic equilibrium, and individual points above correspond to χ's inferred from W/Re-hydrogen dissociation experiments (Sec. IV B 1).

phase equilibrium, but were consistent with predictions from epicatalysis.

The apparatus consisted of a stainless steel cylindrical vacuum vessel (40 cm high, 30 cm diameter; Fig. 5). Two ribbon filaments (W vs Re, 8 cm × 2.5 mm × 0.03 mm; and W vs Mo, 6 cm × 2.5 mm × 0.03 mm) were dc Ohmically heated ($300 \leqslant T \leqslant 2500$ K) in a constant pressure atmosphere (either vacuum, pure He, or pure H_2; $10^{-6} \leqslant \mathcal{P} \leqslant 30$ Torr). Electrical dc power was supplied to the filaments to achieve a fixed temperature against the several possible energy loss channels (e.g., convection, conduction, radiation, H_2 dissociation). Temperature was measured with a calibrated optical pyrometer, and gas pressure was measured using calibrated capacitance manometer gauges.

The power consumed by a filament dissociating hydrogen, P_{hd}, as well as its other loss channels, was inferred by running the filament at a fixed temperature first in vacuum, then in He, and lastly in H_2, the latter two at identical pressures, following the protocol of Jansen *et al.* [10]. A filament's power consumption in vacuum, P_{vac}, was due strictly to
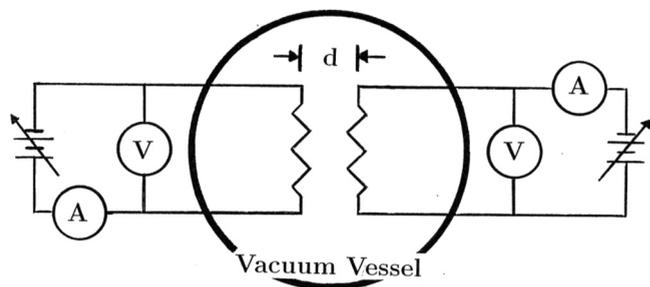

FIG. 5. Schematic of experimental apparatus for hydrogen dissociation experiments [11]. Filaments are symbolized by resistors.

radiation losses ($P_{rad} = \epsilon \sigma T^4 A_{filament}$) and to heat conduction from the hot filament to the copper electrodes holding it: $P_{vac} = P_{rad} + P_{cond}$. Because the filament pairs had identical dimensions and comparable spectral emissivities and coefficients of thermal conductivity, their radiative and conductive losses were similar. When the filaments were heated in He the convection loss channel ($P_{conv,s}$) was added. The convective power consumption were inferred by subtracting P_{vac} from the total power consumption in He; that is, $P_{conv} = P_{He} - P_{vac}$. Helium was used because its thermal conductivity is similar to that of H_2 and, therefore, can be used to estimate the convective losses due to H_2.

Lastly, from the power loss in a H_2 atmosphere (P_{H_2}), the power consumption due to hydrogen dissociation, P_{hd}, was estimated from $P_{hd} \simeq P_{H_2} - P_{He}$. Properly included in P_{H_2} for higher temperatures ($T \gtrsim 1700$ K) are additional convection terms ($P_{conv,a}$) associated with excitation of rotational and/or vibrational modes of H_2 and the additional heat capacity arising from the generation of 2H from a single H_2. Estimates indicate that these contributed 10% or less to P_{hd} [10]. The relative smallness of $P_{conv,a}$ can be estimated by considering the ratio of H-H bond energy ($E_b = 4.47$ eV) to the equipartitioned thermal energy ($\sim kT \sim 0.17$ eV, for $T = 2000$ K). This ratio is $\frac{E_b}{kT} = \frac{4.47}{0.20} \simeq 26$.

A high degree of physical symmetry was built into the apparatus in order to assure that conductive, convective, and radiative losses were as similar as possible for both filaments. The filaments, manufactured to identical physical dimensions, were placed symmetrically at the center of the vacuum vessel. The copper electrodes holding the filaments, as well as their lead wires, were identical in design and placement. The power supplies, ammeters, and voltmeters for both filaments were identical models and were calibrated against each other and against a third, fiducial instrument.

(a) Tungsten vs molybdenum [11]. In Fig. 6(a) is plotted the hydrogen dissociation power (P_{hd}) versus temperature for Mo and W filaments heated singly at 2.5 Torr pressure H_2. The consistently greater power consumed by the Mo establishes that the surface dissociation rate on Mo was greater than on W. It also indicates that the gas concentrations of H and H_2 over Mo and W could not both have been at equilibrium values because gas phase equilibrium concentrations are unique at a given temperature and pressure. In fact, based on power consumption, pressure, and filament dimensions, analysis indicates that the gas phase hydrogen atom concentrations exceeded those predicted under thermal equilibrium by at least an order of magnitude.

In Fig. 6(b) is plotted the difference in P_{hd} between Mo and W per Torr H_2, that is, $\frac{\Delta P_{hd}}{\mathcal{P}(H_2)} \equiv \frac{P_{hd}(Mo) - P_{hd}(W)}{\mathcal{P}(H_2)}$ versus H_2 partial pressure, $\mathcal{P}(H_2)$. At low pressures [$\mathcal{P}(H_2) \leqslant 10$ Torr], based on the criteria for epicatalysis, one expects surface-specific reaction and desorption rates to dominate such that $\Delta P_{hd}/\mathcal{P}$ should be relatively large. The data show this. The nonzero values of $\Delta P_{hd}/\mathcal{P}$ at low pressure indicate both nonequilibrium gas phase concentrations and also substantially larger surface dissociation rates on Mo than on W. In contrast, at high pressures, three-body recombinative mean free paths become relatively short so gas phase reactions should dominate, and gas phase equilibrium should be approached over both
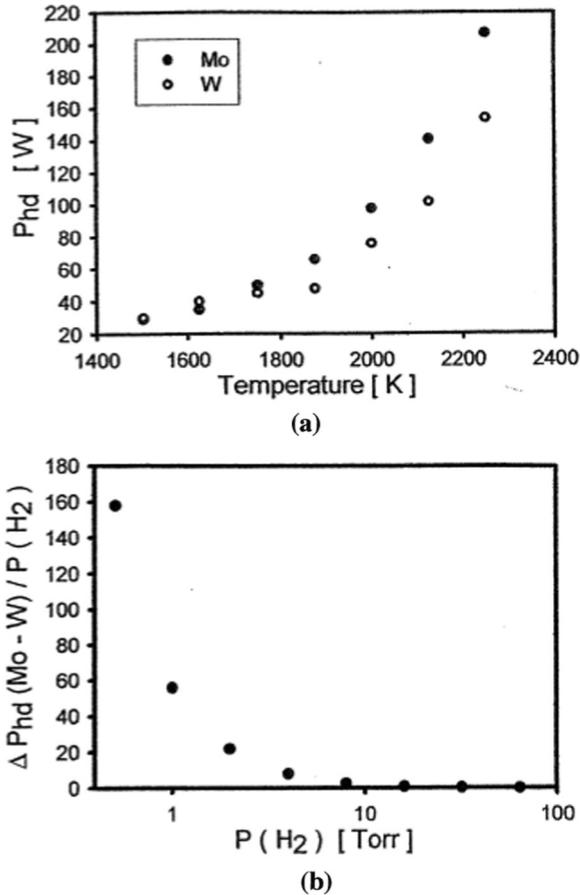
FIG. 6. Hydrogen dissociation on Mo and W filaments: (a) Hydrogen dissociation power (P_{hd}) versus filament temperature for W and Mo filaments. [$\mathcal{P}(H_2) = 2.5$ Torr.] (b) Difference in P_{hd} per Torr ($\Delta P_{hd}/\mathcal{P}$) versus hydrogen pressure for W and Mo filaments ($T = 2200$ K) [11].

surfaces. The chemical differences between Mo and W should be obviated, and $\Delta P_{hd}/\mathcal{P}$ should decrease to zero, also indicated in Fig. 6(b). Other gas-surface systems show similar behavior (Sec. IV B2).

(b) Tungsten vs rhenium [31]. In experiments modeled on those on W-Mo above, similarly distinct surface dissociation rates were also observed between tungsten and rhenium surfaces. When heated to identical temperatures and under identical hydrogen pressures, Re displayed significantly greater (up to two times greater) H_2 dissociation rates than W, and showed similar pressure and temperature trends as seen with W and Mo.

The W and Re filaments were operated on a limited basis at very low pressures ($P \lesssim 20$ mTorr) to compare their absolute gas-surface reaction rates and to quantify their deviations from gas phase equilibrium. Whereas previous experiments operated in the diffusive regime ($P > 1$ Torr), here the two-body and three-body collision mean free paths (λ_2 and λ_3) exceeded the length scales of the filaments so atoms behaved ballistically, interacting with the filaments roughly once before exiting the reaction region. The gas phase processes leading to gas phase equilibrium were eliminated so the gas-surface reaction rates could be laid bare.

Tungsten and rhenium filaments were heated to 1800 K at $\mathcal{P}(H_2) = 10$ mTorr. Gas phase equilibrium (Fig. 4) predicts the dissociation ratio χ_H(GPE) = 0.0004. Hydrogen power consumption on Re and W filaments indicated that hydrogen dissociation ratios above their surfaces were χ_H(Re) = 0.04 and χ_H(W) = 0.02. These results indicate that surface-mediated dissociation ratios for W and Re are both distinct from each other and are 50–100 times greater than those predicted from gas phase equilibrium. It can be shown analytically that, were blackbody cavities constructed exclusively from these metals, gas phase equilibrium could not develop inside them. In other words, they would house stationary-state nonequilibrium gas phase concentrations of H and H_2, closely approximating limiting case 2 from Sec. III. Laboratory examples of these W-Re blackbody cavity systems have been realized, and they verify the predicted stationary-state nonequilibrium [33].

2. Corroborative hydrogen-metal experiments

Other researchers have reported similar findings to those described above, although they were not investigating epicatalysis *per se*. Close reading of their texts reveals surprise and unease with their results, as they struggle to explain their anomalously high H atom concentrations, which are at odds with thermodynamic equilibrium and their transport models.

(a) Otsuka et al. [34]. Otsuka *et al.* investigated and compared hydrogen dissociation on W and Ta filaments. The following is the text of their abstract in its entirety [34].

> "The electric power consumed by hot tantalum and tungsten filaments used to dissociate hydrogen molecules into hydrogen radicals was measured at filament temperatures of 2000, 2300, and 2500 °C and hydrogen pressures from 0.5–100 Torr. The measured power consumption at pressures above 30 Torr was well represented by a model that assumed thermodynamic equilibrium between the H_2 and H near the filament. With decreasing pressure, however, the dissociation of H_2 shifted from an equilibrium-controlled regime to a surface-reaction-rate-controlled regime. The relationship between the power consumption and the pressure in the surface-reaction-rate-controlled regime was correlated with the surface dissociation probability, which was determined to range from 0.18 to 0.94."

Their "surface-reaction-rate-controlled regime" is evidence of epicatalysis. In this regime they find that the surface dissociation probability (η) increases with temperature and is distinct between Ta ($0.16 \leqslant \eta$(Ta) $\leqslant 0.62$) and W ($0.18 \leqslant \eta$(W) $\leqslant 0.94$) over identical temperature and pressure ranges. That different species concentrations prevail over the two metals, at otherwise identical pressures and temperatures, is one of the signatures of epicatalysis.

Based on Arrhenius plots, Otsuka *et al.* "determined the activation energy of H_2 dissociation on tantalum to be 21.3 (kJ/mole) and for tungsten to be 22.9 (kJ/mole)." They also "note that the data for tantalum does not follow a simple Arrhenius form, however, and may be better represented by a modified Arrhenius equation with higher-order temperature

dependence." It is mysterious that these reported activation energies are an order of magnitude smaller than what is expected thermodynamically for hydrogen dissociation, or even more charitably, simply desorption energy. The minimum activation energy for the reaction $H_2(g) + M \longrightarrow 2H(g) + M$, where M is the metal, should be roughly half the bond energy for gas phase dissociation ($432/2 = 216$ kJ/mole). They are not the only researchers to observe anomalously low activation energies for hydrogen dissociative desorption [35].

(b) Jansen et al. [10]. Jansen *et al.* [10] investigated hydrogen and deuterium dissociation on Re wires, systematically varying wire diameter, temperature, and gas pressure. They observe:

> "a dissociation rate of the hydrogen gas that is more than one order of magnitude higher than the equilibrium dissociation . . . . One would expect these effects to become important when the wire size is of the order of the mean free path of the hydrogen molecule or atom. It is surprising that the effects are observable with wires that are many times larger in diameter than the estimated mean free path (i.e., of the order of several tens of micrometers at a few thousand degrees kelvin)."

What Jansen *et al.* consider "surprising" is understandable in the context of epicatalysis. The long mean free path for recombinative three-body collisions (λ_3) delays the gas phase equilibrium well beyond the two-body collision length (λ_2). The reaction mean free path λ_{Rx} should be at least $\lambda_{Rx} = \sqrt{\lambda_2\lambda_3}$ and, probably, many times longer; thus, even taking radially asymmetric diffusion into account, their results favor epicatalysis.

(c) Schäfer et al. [36]. Quoting from their article abstract, the authors make "quantitative determination of atomic hydrogen concentrations in the vicinity of hot filaments ...with two-photon laser-induced fluorescence." They find that "H concentration profiles for Ta, Ir, and W filaments show a dependence on filament materials," amplifying the findings of Otsuka *et al.* [34] and Sheehan *et al.* [11,31]. Traditional catalysts cannot alter the thermodynamic equilibrium over their surfaces so even if Schäfer *et al.* were operating in a diffusion-controlled regime, as argued by Jansen *et al.* [10], they were probably observing epicatalysis because, unlike traditional catalysts, epicatalysts permit (and predict) distinct gas species concentrations over chemically distinct surfaces.

(d) Qi et al. [35]. The most explicit acknowledgment of anomalous nonequilibrium effects was made by Qi *et al.*, who compiled and analyzed the results of several previous hydrogen surface-dissociation studies. In analyzing experiments by one group of researchers [37], they concluded that gas species concentrations are 20 times larger than can be explained by gas phase equilibrium. They state, "Thus, gas-phase chemistry cannot account for the measured concentrations of H radiation." In their Conclusions, they state:

> "Heterogeneous chemistry at the filament is the dominant source of atomic hydrogen and gas-phase chemistry plays a negligible role. Arrhenius plots of hydrogen dissociation rates on the refractory filament surface ...yield effective activation

energy much lower than that of homogeneous thermal decomposition of molecular hydrogen."

Their Arrhenius plots yield the following activation energies for hydrogen dissociative desorption (in kJ/mole): TaC (100), Ta (105), Re (118), and W (157 and 166). They are considerably less than the minimum expected value of 216 kJ/mole.

In summary, several research groups over the last 25 years have noted anomalously high and surface-specific hydrogen atom concentrations over high-temperature refractory materials that cannot be easily explained through equilibrium thermodynamics and standard catalysis, but which are consistent with epicatalysis. Their experiments corroborate those specifically designed to quantitatively measure epicatalytic effects [11,31].

V. DISCUSSION AND OUTLOOK

At present, epicatalysis appears limited to high-temperature and low-pressure regimes; however, there are good reasons to expect that its thermodynamic range can be broadened considerably. All surfaces and gases are physically or chemically active to some degree. Surface ionization and surface dissociation of covalently bonded diatomic molecules like hydrogen (e.g., N_2, O_2, F_2, Cl_2) involve significant ionization, bond, and desorption energies; therefore, these types of epicatalysis are probably confined to high temperatures. Lower-energy reactions, however, should imply lower temperatures. Surface isomerization of organics, for example, involve intramolecular rearrangements that do not necessarily involve significant net enthalpy changes, so gas-surface bonds can be of lesser strength, not requiring full covalent character; thus, these reactions should proceed at lower temperatures. Indeed, the catalytic isomerization of *n*-butane to isobutane proceeds at less than 400 K. Likewise, multiadsorbate processes (e.g., Langmuir-Hinshelwood style hydrogenation, oxidation, carbonylation, and halogenation) might have large heats of formation, but if their desorption energies are low, they are likely to proceed at moderate or low temperatures as well.

Proceeding to even lower temperatures, hydrogen-bonded dimers, like those of formic acid [$(HCOOH)_2$] and ammonia [$(NH_3)_2$], are bound by much weaker (hydrogen) bonds [38]; therefore, bond-breaking gas-surface interactions should be commensurately weaker and the reaction temperature lower. Polar or dielectric (polarizable) surfaces—ones not necessarily forming covalent bonds with adsorbate—should suffice for dissociation. Desorption should proceed at much lower temperatures than for covalent-bond reactions, perhaps near room temperature.

The connection between reaction energy, desorption energy, and epicatalytic operating temperature can be argued based on energy scaling [39]. An equilibrium constant depends on temperature and reaction Gibbs free energy ($K_{eq} = \exp[-\Delta G/RT]$), whose most prominent contribution is typically the bond energy for the reaction. If so, the characteristic energy scale for chemical equilibrium is $\frac{\text{bond energy}}{\text{thermal energy}} = |\frac{\Delta G}{RT}| \equiv \phi$. Energy scaling indicates that weaker bonds would require commensurately lower temperature to achieve similar levels of dissociation and desorption. Hydrogen bonds (~ 0.5 eV) are typically an order of magnitude weaker than covalent bonds

($\sim$5 eV), and van der Waals bonds an order of magnitude weaker still ($\sim$0.05 eV). Thus, if covalent epicatalysis of H_2 proceeds well at 2000–3000 K, epicatalytic dissociation of hydrogen-bonded dimers might proceed well at or below room temperature; that is, $\phi(4.5 \text{ eV}/2000 \text{ K}) \simeq \phi(0.5 \text{ eV}/220 \text{ K})$. In other words, the phenomenon of epicatalysis is probably not confined to high temperatures.

Criterion 2 for epicatalysis, which requires that the gas phase be chemically inert, can be arranged by ensuring that the mean free paths for gas phase reactions remain long or comparable to the distance between gas-surface collisions, i.e., $\lambda_{Rx} \gtrsim L$. For the macroscopic epicatalytic systems this is ensured by keeping the volume number densities low, but this condition is not required. Epicatalysis can operate at high number densities and pressures if the wall-to-wall distance (L) is sufficiently small.

For discussion, let the benchmark length for reactions be the two-body mean free path [40], that is, let $\lambda_{Rx} = \lambda_2 \sim \frac{1}{n\sigma}$. For the experiments documented in Sec. IV, the system scale sizes were small but macroscopic ($L \simeq 10^{-2}$ m), and the pressures were low, less than 5×10^{-2} atm ($n \lesssim 10^{24}$ m^{-3}). Due to their inverse relationship, if the distances between epicatalytic surfaces are reduced then the number densities can be proportionately increased, while still satisfying criterion 2. In practical terms, this means that by reducing the distances of epicatalytic surfaces from centimeters down to microns or tens of nanometers, viable pressures can be raised from milliTorrs up to tens or perhaps hundreds of atmospheres. Epicatalysis, then, seems well suited to micro- and nanoscale heterogeneous chemistry because at this scale criterion 2 is naturally satisfied, even at high pressures.

Together, energy and size scaling suggest that epicatalysis should be viable from below room temperature up to the melting points of refractory metals, from the lowest possible pressures up to hundreds of atmospheres. Also, because criteria 1 and 2 are quite general, it should apply to many types of heterogeneous reactions.

Thus far, the discussion has been restricted to heterogeneous reactions at surfaces only, but it is plausible that epicatalysis might be viable—even enhanced—with materials into which gases can dissolve. Hydrogen, for instance, is soluble to some degree in all metals, and some are renowned for their storage capabilities (e.g., Pd,Ti). Light molecules like O_2 and N_2 are also known to dissolve in metals. These possibilities might be expanded to include dendritic and zeolitic structures, and perhaps porous plugs, which have been explored as hotplates in Q machines [7]. Bulk solvation, diffusion, and dissociation should promote epicatalysis and perhaps even lower its operating temperature by providing favorable entropy changes. Further discussion lies beyond the scope of this paper.

Epicatalysis has a number of potential strengths and limitations. As one might expect, these are rooted in its two criteria. Whereas traditional catalysts are constrained by chemical equilibrium, epicatalysts are not; thus, it is possible to obtain from them product streams enriched in desirable nonequilibrium products. For example, in epicatalytic hydrogen atom sources, (desirable) hydrogen radical concentrations have been measured to be up to 100 times greater than those allowed under thermal equilibrium. In principle, epicatalytic product streams might even contain species forbidden by

equilibrium thermodynamics, thereby opening the door to additional synthetic routes and products.

Epicatalysis offers a further control parameter for heterogeneous chemical reactions: of surface type. Rather than relying solely on temperature and pressure to set gas phase concentrations (or other parameters consistent with the Gibbs phase rule), surface chemical properties can now be used to steer reactions beyond the normal boundaries of thermodynamic equilibrium. Operationally this means that, starting with the same reactants at identical pressure and temperature, in principle, a reaction can be guided to different end products and concentrations, simply by tailoring the surface composition of the reaction vessel.

Epicatalysts can generate gas concentration profiles that mirror profiles obtainable only at considerably higher temperature under thermal equilibrium. In practical terms, this might reduce the temperature, power requirements, complexity, and costs associated with some processes. For instance, in order to achieve the hydrogen dissociation ratio seen epicatalytically from Re at just 1800 K (Sec. IV), a gas at thermal equilibrium would have to be heated to about 2600 K (see Fig. 4). At 2600 K the gas would be more ionized, hence the hydrogen stream would be more contaminated with plasma. Hydrogen epicatalysts, in contrast, not only provide low-temperature routes to a high-temperature species profile, they might also require less power and less apparatus than a purely thermal source, while simultaneously providing a more pristine, less contaminated product stream of hydrogen radicals. This should extend to the production of other light radicals from dimeric parents [e.g., $O_2, N_2, Cl_2, (CN)_2$].

Epicatalysis, by virtue of its nonequilibrium nature, offers a potent way to boost the thermochemical energy of reaction products. Again, consider hydrogen dissociation. Under specific conditions ($T = 1800$ K; $P = 10$ mTorr), the gas phase dissociation ratio is predicted to be $\chi_H \simeq 4 \times 10^{-4}$ at thermal equilibrium, while the epicatalytic dissociation ratio over Re was experimentally inferred to be 100 times larger ($\chi_H \simeq 0.04 = 1/25$). Given that the hydrogen covalent-bond energy (4.5 eV) is roughly 25 times greater than the thermal energy (kT) at $T = 1800$ K, and given that the epicatalytic dissociation ratio was roughly $\chi_H \simeq 1/25$, it follows that the total thermochemical energy ($E_{bond} + kT$) of the product stream was roughly twice as large as that permitted under thermodynamic equilibrium. (The excess energy is primarily due to anomalously high H-radical concentrations.) In other circumstances, this excess thermochemical energy might be manifested as higher-temperature products or added, thermodynamically forbidden bonds.

By transcending some of the constraints of equilibrium thermodynamics, epicatalysts might help realize some of the aspirations of green chemistry [5,41], in particular, they might (i) prevent waste by obtaining better yield with less feedstock; (ii) provide different synthetic routes with less toxic reagents; (iii) minimize use of auxiliary reagents and solvents; and (iv) reduce energy use. Each of these goals is either directly demonstrated or strongly suggested by the hydrogen-metal experiments (Sec. IV), which exhibited high product yield (H radicals) at relatively low temperature (1800 versus 2600 K), and offered higher thermochemical energy content than could be achieved via thermal equilibrium

dissociation. Also, the apparatus was nontoxic, simple, and relatively inexpensive (Fig. 5). In sum, epicatalysts "stretch out" heterogeneous reactions in both space and time, liberating into the gas phase ephemeral, nonequilibrium species that are normally confined to the surface. In doing so, they expand the palette and possibilities of catalytic chemistry beyond the normal limits set by equilibrium thermodynamics.

Epicatalysis also has several potential limitations. First, it appears susceptible to all the ills that plague regular heterogeneous catalysis, among which are surface contamination and physical degradation, grain sintering, fouling, coking, and poisoning. As for catalysts, some of these failings might be delayed—for instance, by running them at low temperatures, in high vacuum, or by using pure feedstock—while others might be reversed, as with catalyst regeneration schemes [42,43]. Also, as mentioned above, by providing other control parameters in the form of surface reactivity, epicatalysts might also cause unwanted complexity, for instance, by creating deleterious side products.

Criterion 2 will likely make epicatalysis problematic for large-scale commercial use. The long mean-path requirement ($\zeta \gtrsim 1$) will probably limit viable operating pressures of large epicatalytic reactors to values orders of magnitude below those of commercial reactors, thereby limiting product fluxes (and profits) accordingly. If criterion 2 is to be met at high pressure, e.g., by working with microreactors, then the high costs and complexities of microfabrication must be borne. Overall, epicatalysis seems best suited to fast, single-pass reactors in which nonequilibrium gas phase products can be quickly secured, before they succumb to thermal equilibrium.

Lastly, epicatalysis might have relevance in certain astrophysical settings, for instance, in molecular clouds or protoplanetary nebulae with dust or ice grains; comet tails; the rings of the giant gas planets; or around refractory grains in the outer atmospheres of stars. Most of these are probably too cold to drive reactions thermally to a significant degree, but most have other, superthermal drivers (e.g., uv radiation, plasmas, or energetic electrons or protons) that might suffice. A deeper discussion is beyond the scope of this paper, but it will be interesting to see if epicatalysis can be found outside the laboratory.

Historically, catalysis has been understood almost exclusively under the rubric of thermodynamic equilibrium. Epicatalysis helps change this by pushing heterogeneous catalysis into the less studied nonequilibrium regime. Kinetic theory clearly predicts its existence and well-studied experimental systems unambiguously demonstrate it. Extrapolating from these, it appears that other epicatalytic systems are waiting to be discovered, and numerous applications might be on the horizon. To summarize and conclude: *Catalysts alter the kinetics but not the thermodynamics of reactions; epicatalysts alter both.*

[1] V. Parmon, *Thermodynamics of Non-Equilibrium Processes for Chemists with a Particular Application to Catalysis* (Elsevier, Amsterdam, 2010).

[2] K. W. Kolasinski, *Surface Science: Foundations of Catalysis and Nanoscience*, 2nd ed. (John Wiley, West Sussex, England, 2009).

[3] R. I. Masel, *Principles of Adsorption and Reaction on Solid Surfaces* (John Wiley, New York, 1996).

[4] S. Kauffman, *At Home in the Universe: The Search for the Laws of Self-Organization and Complexity* (Oxford University Press, Oxford, 1995).

[5] G. Rothenberg, *Catalysis: Concepts and Green Applications* (Wiley-VCH, Weinheim, 2008).

[6] V. Smil, *Enriching the Earth: Fritz Haber, Carl Bosch and the Transformation of World Food Production* (MIT Press, Cambridge, MA, 2001).

[7] R. W. Motley, *Q-Machines* (Academic Press, New York, 1975).

[8] N. Rynn and N. D'Angelo, Rev. Sci. Instrum. **31**, 1326 (1960).

[9] I. Langmuir, J. Am. Chem. Soc. **34**, 860 (1912); **34**, 1310 (1912).

[10] F. Jansen, I. Chen, and M. A. Machonkin, J. Appl. Phys. **66**, 5749 (1989).

[11] D. P. Sheehan, Phys. Lett. A **280**, 185 (2001).

[12] I. Langmuir and K. H. Kingdon, Proc. R. Soc. London, Ser. A **107**, 61 (1925).

[13] M. Kaminsky, *Atomic and Ionic Impact Phenomena on Metal Surfaces* (Academic, New York, 1965).

[14] The Saha equation was originally inspired by diatomic molecular dissociation. Fittingly, the same kinetic formalism can be applied to it as is developed in Sec. III Eq. (1), simply by substituting "ionization" for "dissociation."

[15] R. C. Knechtli and J. Y. Wada, Phys. Rev. Lett. **6**, 215 (1961).

[16] S. von Goeler, Phys. Fluids **7**, 463 (1964).

[17] Gas phase recombination (deionization) proceeds primarily via the following three-body channel: $M^+ + e^- + e^- \longrightarrow M + e^-$.

[18] N. I. Ionov, Zh. Eksp. Teor. Fiz. **18**, 174 (1948) [J. Exp. Theor. Phys. **18**, 174 (1948)].

[19] S. Datz and E. H. Taylor, J. Chem. Phys. **25**, 389 (1956).

[20] F. C. Tompkins, *Chemisorption of Gases on Metals* (Academic Press, London, 1978).

[21] R. J. Madix and J. T. Roberts, in *Surface Reactions*, edited by R. J. Madix, Springer Series in Surface Sciences Vol. 34, (Springer-Verlag, Berlin, 1994).

[22] More precisely, L is the physical size scale of the chamber (l_c) normalized by the accommodation coefficient for surface adsorption (α); that is, $L = l_c/\alpha$. For perfect adsorption by the walls ($\alpha = 1$), one has $L = l_c$. (Going forward, $\alpha = 1$ will be assumed.)

[23] R. H. Fowler and E. A. Milne, Proc. Natl. Acad. Sci. U.S.A. **11**, 400 (1925).

[24] R. C. Tolman, Proc. Natl. Acad. Sci. U.S.A. **11**, 436 (1925).

[25] P. Clausing, Ann. Phys. (Leipzig) **4**, 533 (1930).

[26] *NIST-JANAF (Joint Army Navy and Air Force), 4th edition*, edited by M. W. Chase, Jr. (American Institute of Physics, Melville, NY, 1998).

[27] N. Cohen and K. R. Westberg, J. Phys. Chem. Ref. Data **12**, 531 (1983).

[28] W. F. Sheehan, *Chemistry: A Physical Approach* (Allyn and Bacon, Boston, 1964), p. 501.

[29] D. P. Sheehan and T. Seideman, J. Chem. Phys. **122**, 204713 (2005).

[30] D. P. Sheehan, Phys. Plasmas **3**, 104 (1996).

[31] D. P. Sheehan, J. T. Garamella, D. J. Mallin, and W. F. Sheehan, Phys. Scr., T **151**, 014030 (2012).

[32] D. P. Sheehan, Phys. Rev. E **57**, 6660 (1998).

[33] D. P. Sheehan (unpublished).

[34] T. Otsuka, M. Ihara, and H. Komiyama, J. Appl. Phys. **77**, 893 (1995).

[35] X. Qi, Z. Chen, and G. Wang, J. Mater. Sci. Technol. **19**, 235 (2003).

[36] L. Schäfer, C.-P. Klages, U. Meier, and K. Kohse-Höinghaus, Appl. Phys. Lett. **58**, 571 (1991).

[37] M. A. Childs, K. L. Menningen, L. W. Anderson, and J. E. Lawler, J. Chem. Phys. **107**, 5918 (1997).

[38] G. Gilli and P. Gilli, *The Nature of the Hydrogen Bond* (Oxford University Press, Oxford, 2009).

[39] D. P. Sheehan, J. T. Garamella, D. J. Mallin, and W. F. Sheehan, in *Second Law of Thermodynamics: Status and Challenges*, edited by D. P. Sheehan, AIP Conf. Proc. No. 1411 (AIP, Melville, NY, 2011), p. 65.

[40] For gas phase hydrogen recombination, three-body collisions are actually required, and these have much longer mean free paths ($\lambda_3 \gg \lambda_2$), which only bolsters the argument.

[41] *Environmental Catalysis*, edited by F. J. J. G. Jannsen and R. A. van Santen, Science Series Vol. 1 (Imperial College Press, London, 1999).

[42] *Deactivation and Regeneration of Zeolite Catalysts*, edited by M. Guisnet and F. Ramôa Ribeiro, Catalytic Science Series Vol. 9 (Imperial College Press, London, 2011).

[43] Time scales for deactivation range from a few seconds (e.g., zeolite processes) to many years (e.g., C_5-C_6 alkane hydroisomerization). Haber-Bosch catalysts hold the record at more than 10 yr.